



HAL
open science

Novel 2D/3D Heterojunction for UV Light-Emitting Diodes Using Hexagonal Boron Nitride as Hole Injection Layer

Andre Perepeliuc, Rajat Gujrati, Phuong Vuong, Vishnu Ottapilakkal, Thi May Tran, Mohamed Bouras, Ali Kassem, Ashutosh Srivastava, Tarik Moudakir, Gilles Patriarche, et al.

► To cite this version:

Andre Perepeliuc, Rajat Gujrati, Phuong Vuong, Vishnu Ottapilakkal, Thi May Tran, et al.. Novel 2D/3D Heterojunction for UV Light-Emitting Diodes Using Hexagonal Boron Nitride as Hole Injection Layer. *Advanced Photonics Research*, 2024, 2400092, pp.1-6. 10.1002/adpr.202400092. hal-04758198

HAL Id: hal-04758198

<https://hal.science/hal-04758198v1>

Submitted on 29 Oct 2024

HAL is a multi-disciplinary open access archive for the deposit and dissemination of scientific research documents, whether they are published or not. The documents may come from teaching and research institutions in France or abroad, or from public or private research centers.

L'archive ouverte pluridisciplinaire **HAL**, est destinée au dépôt et à la diffusion de documents scientifiques de niveau recherche, publiés ou non, émanant des établissements d'enseignement et de recherche français ou étrangers, des laboratoires publics ou privés.

Novel 2-D/3-D heterojunction for UV LEDs using Hexagonal Boron Nitride as hole injection layer

*Andre Perepeliuc, Rajat Gujrati, Phuong Vuong, Vishnu Ottapilakkal, May Tran Thi, Mohamed Bouras, Ali Kassem, Ashutosh Srivastava, Tarik Moudakir, Gilles Patriarche, Paul Voss, Suresh Sundaram, Jean Paul Salvestrini, Abdallah Ougazzaden**

A. Perepeliuc, R. Gujrati, V. Ottapilakkal, M. T. Thi, M. Bouras, A. Kassem, S. Sundaram, J. P. Salvestrini, A. Ougazzaden

CNRS IRL 2958 GT-CNRS 2 Rue Marconi, 57070 Metz, France.

Email: abdallah.ougazzaden@georgiatech-metz.fr

A. Perepeliuc, P. L. Voss, S. Sundaram, J. P. Salvestrini, A. Ougazzaden*

Georgia Institute of Technology School of Electrical and Computer Engineering, Atlanta, USA.

P. Vuong, A. Srivastava, S. Sundaram, J. P. Salvestrini

Georgia Tech – Europe, 2 Rue Marconi, 57070 Metz, France.

T. Moudakir

Institut Lafayette, 3 rue Marconi, Metz, France.

G. Patriarche

Centre de Nanosciences et de Nanotechnologies, Université Paris-Saclay, C2N - Site de Marcoussis, Route de Nozay, F-91460 Marcoussis, France.

Keywords: 2-D/3-D heterojunction, UV LEDs, p-doped hexagonal boron nitride, hole injection layer.

The AlGa_N materials system has been extensively studied in order to improve the efficiency of UV-B and UV-C LEDs. While progress has been made, significant challenges remain at shorter wavelengths. Most notably, increased Al composition for shorter wavelength operation results in increased activation energy of Mg dopants, resulting in low p-doping. Although p-doped h-BN, with a bandgap of 5.9 eV, has been proposed as a potential replacement of p-doped AlGa_N, there have not been demonstrations of LEDs fabricated from p-doped h-BN/AlGa_N heterostructures. Such unique heterostructures combine two dimensional p-doped h-BN materials with three

dimensional AlGa_{0.15}N materials. In this paper we report fabrication and characterization of p-doped h-BN/AlGa_{0.15}N MQW/n-AlGa_{0.15}N LEDs, demonstrating emission of light at 290 nm corresponding to the AlGa_{0.15}N MQWs, with weaker emission at 262 nm corresponding to the AlGa_{0.15}N barrier. These results conclusively show hole injection through p-doped h-BN into AlGa_{0.15}N and provide a proof-of-concept that p-doped h-BN can be an alternative hole injection layer for UV LEDs.

1. Introduction

After two decades of dedicated research and a host of improvements, challenges remain for aluminum gallium nitride (AlGa_{0.15}N)-based ultra violet light emitting diodes (UV-LEDs)^[1]. This performance gap between AlGa_{0.15}N and GaN LEDs is attributed to various factors, such as threading dislocations originating from the aluminum nitride (AlN)/sapphire interface, which reduce internal quantum efficiency^[2] as well as a contact layer opaque to UV light, diminishing extraction efficiency. For shorter wavelengths, doping remains the largest problem. While researchers have achieved success in growing highly doped and conductive n-AlGa_{0.15}N layers (doping = $1.5 \times 10^{19} \text{cm}^{-3}$, resistivity = $0.026 \ \Omega \ \text{cm}$ in n-Al_{0.81}Ga_{0.19}N)^[3], the p-doping of AlGa_{0.15}N still presents a major challenge due to presence of compensating nitrogen vacancy point defects^[4] and the high activation energy of magnesium (Mg) dopants, which reaches several hundreds of meV^[5] for high Al-content AlGa_{0.15}N.

Efforts to reduce compensation and activation energy of Mg dopants in p-AlGa_{0.15}N spurred the exploration of various innovative solutions. On one hand, researchers have investigated flow rate modulation techniques such as Mg-delta doping^[6] and Mg-Si co-doping^[7], to enhance the hole concentration of Mg-doped p-AlGa_{0.15}N. On the other hand, researchers have investigated various Mg-doped structures such as AlGa_{0.15}N/GaN super lattice (SL)^[8], AlGa_{0.15}N/AlN/GaN multi-heterostructures^[9] and multidimensional SL^[10], which leverage polarization induced charges to

achieve efficient p-doping. In parallel, other method such as polarization engineered p⁺-AlGa_N/InGa_N/n⁺-AlGa_N tunnel junction^[11], n⁺-Ga_N/Al/p⁺-AlGa_N nanowire based tunnel junction^[12] and use of p-Si/Al₂O₃/p-Ga_N^[13] has also been proposed for efficient hole injection in UV-LEDs. Finally, for far UV emission, a few researchers have attempted to push AlGa_N to the limits of its band gap by fabricating AlN p-n homojunctions^[14,15]. Despite these attempts, the external quantum efficiency (EQE) of UV-LEDs remains significantly low, scarcely surpassing 1% at 230 nm emission^[16], dropping to 0.003% at 222 nm emission^[17] and finally plummeting to 10⁻⁶ % for AlN homojunctions^[15].

Against the backdrop of these challenges, there is growing demand for compact and efficient UV sources. This demand is propelled by a variety of applications including skin antiseptics^[18], non-line-of-sight communications^[19], water disinfection^[20], and gas sensing^[21]. Interest in the far UV-C portion of the spectrum, has never been higher. Research indicates that wavelengths below 240 nm can achieve pathogen inactivation while posing 10 times lower risk of harm of human skin^[22], positioning far UV-C sources as the main building block for skin-friendly antiseptic systems. Given these needs, and the technological situation, novel hole injection layers should be investigated.

Over the past decade, hexagonal boron nitride (h-BN), a two-dimensional (2-D) material, has been proposed as a candidate material for UV photonics^[23]. The ultra-wide bandgap of 5.995eV^[24] positions h-BN as a UV-transparent current-injecting layer, so that UV-blocking p-Ga_N contact layers are not needed, which enhances photon extraction efficiency. Additionally, the high electron band offset of h-BN with AlGa_N^[25] blocks electrons, thus eliminating the requirement for the resistive AlGa_N/AlN electron blocking layers (EBL) typically used in UV-C LEDs. Therefore, h-BN has been proposed as a novel hole injection layer in UV-LEDs.

Recent reports include improvements in the epitaxy of wafer-scale Mg-doped p-BN through metalorganic chemical vapor deposition (MOCVD)^[26,27]. Researchers have reported free hole concentration, resistivity and mobility equal to $1.1 \times 10^{18} \text{cm}^{-3}$, $0.5 \text{cm}^2/\text{V/s}$ and $12 \Omega \cdot \text{cm}$, respectively, in Mg-doped p-BN. Furthermore, the successful attainment of h-BN growth on 6" wafers through MOCVD^[28] signifies a step towards future industrial production of h-BN for UV photonics. Recently, a novel photoinduced doping method for achieving both p- and n-doping of h-BN has been demonstrated^[29,30]. Regarding heterostructures, Majety et al^[23] have reported the first building block by using h-BN in a Mg-doped h-BN/n-AlGaN electrical heterojunction.

However, there have yet to be reports, to the best of our knowledge, of functioning UV-LEDs using Mg-doped h-BN. We believe that this stems from the challenges associated with the growth of Mg-doped h-BN on top of AlGaN multi quantum wells (MQWs). The high temperature needed for growth of thick Mg-doped h-BN risks damaging the integrity of ultra quantum wells (QWs), and the Mg-doped h-BN layers also need to avoid delamination as it is not chemically bonded to the AlGaN layer.

In this work, we report epitaxial growth of 2-D/3-D UV-LED heterojunctions with a p-layer composed of p-type h-BN, fabricated into a working LED. Characterization of the fabricated devices corresponds to the electrical characteristics of a diode and the devices emit UV radiation centered 290 nm with secondary weaker emission at 262 nm. These results demonstrate the proof-of-concept that Mg-doped h-BN could subsequently be integrated into structures with QWs emitting at lower wavelengths, thereby underlining the need for significant research into this technological alternative to AlGaN p-layers.

2. Results and Discussion

2.1 Materials Growth and Characterization

2-D/3-D UV-LED epilayers, Mg-doped h-BN/AlGaN MQW/n-AlGaN/AlN, were grown on a sapphire substrate. As a first step, a 200 nm thick AlN buffer was grown on an epi-ready sapphire substrate. This was followed by the growth of 500 nm thick Si-doped n-Al_{0.57}Ga_{0.43}N and 5-period Al_{0.59}Ga_{0.41}N (13.5 nm)/Al_{0.38}Ga_{0.62}N (2.2 nm) MQWs. Finally, Mg-doped h-BN cap layer was grown at 1280°C and 90 mbar^[31]. Samples, for reasons explained later in manuscript, corresponding to two different thickness of Mg-doped h-BN, 300 nm and 50 nm, were grown. All other underlayers beneath Mg-doped h-BN were kept identical for both samples.

At first, to understand the effect of high temperature growth of Mg-doped h-BN on the underlying MQWs, high resolution transmission electron microscopy (HR-TEM) studies were conducted. Especially, the LED structure, featuring a 300 nm thick Mg-doped h-BN layer was chosen, for HR-TEM inspection.

The cross-section of the full sample (Figure 1a) confirms the presence of 300 nm thick Mg-doped h-BN layer atop the AlGaN MQW/n-AlGaN stack, grown atop of AlN buffer layer. As depicted in Figure 1b, the as-grown 300 nm thick Mg-doped h-BN exhibits a layered structure and retains its hexagonal crystallography for the initial ~50 nm, after which it enters a continuous turbostratic growth phase. Furthermore, Figure 1c reveals that the bottom four QWs are well-preserved and exhibit clear contrast with the quantum barriers (QBs) due to differences in their aluminum content. However, the topmost QW shows some degree of undesired homogenization of aluminum content, attributable to the thin barrier separating the top well and the Mg-doped h-BN layer.

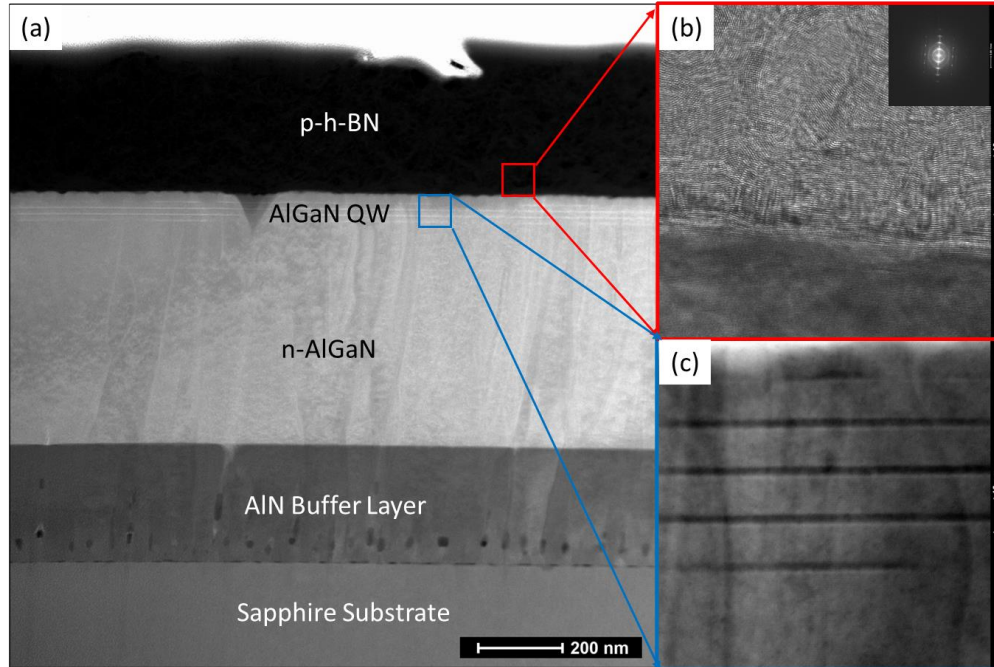


Figure 1. (a) Cross sectional HR-TEM image of the full UV LED structure with Mg-doped h-BN. (b) Magnified dark field image of Mg-doped h-BN epilayer showing the layered and turbostratic growth of Mg-doped h-BN (inset: acquired FFT pattern). (c) Dark field image of the MQWs.

Informed by the insights gleaned from these TEM micrographs, and driven by two key considerations - first, the observed turbostratic growth phenomenon at higher Mg-doped h-BN thicknesses, and secondly, the desire to maintain a lower thermal budget at the topmost QW - we conclude second set UV-LED structure featuring a thinner layer of Mg-doped h-BN must have enhanced epitaxial quality. Thus, we proceeded to delve deeper into our investigation, focusing specifically on UV-LED samples featuring a mere 50 nm thickness of Mg-doped h-BN. The schematic representation of the entire epitaxial stack employed in our subsequent analyses is depicted in Figure 2a.

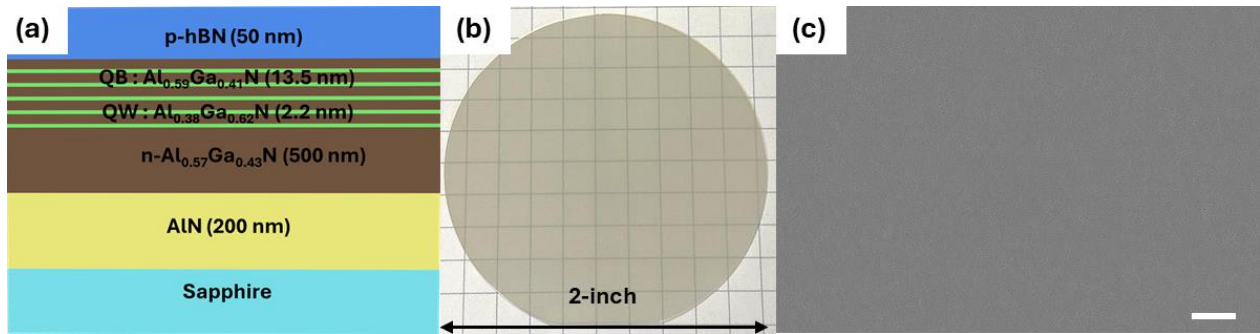


Figure 2. (a) Epilayer stack of the UV LED structure grown (b) Full 2-inch wafer after the growth (c) SEM micrograph of top Mg-doped h-BN epilayer after full structure growth, scale bar 5 μm .

The entire 2" wafer, after the complete growth of the UV-LED structure as shown in Figure 2b, appeared transparent and exhibited a smooth and specular appearance. The Scanning Electron Microscopy (SEM) micrograph of the top Mg-doped h-BN layer is presented in Figure 1c, illustrating characteristic h-BN wrinkles, albeit with shorter-range order compared to hBN grown on sapphire. The characteristic morphology of Mg-doped h-BN, as observed, stems from the underlying AlN buffer layer.

To assess the crystalline quality of the grown epilayers, the high resolution X-Ray diffraction (HR-XRD) measurement performed on the full UV-LED structure and the obtained 2θ - ω plot is shown in Figure 3a. The figure illustrates four distinct diffraction peaks: the (0002) peak of the Mg-doped h-BN, the (0002) peak of n-AlGa_{0.57}N, the (0002) peak of AlN, and the (0006) peak of the sapphire substrate. Additionally, satellite diffraction peaks are clearly observable, indicating the presence of the MQWs. The obtained 2θ - ω scan was fitted considering 80% relaxation of the n-AlGa_{0.57}N epilayer. For the obtained fit, parameters used were found to be in good agreement with epitaxial growth parameters. Al content in QW was found to be 0.38 (± 0.015) with a thickness of 2.2 nm

(± 0.2 nm), while the AlGaIn QB contained 0.57 (± 0.015) Al with a thickness of 13.5 nm (± 0.2 nm).

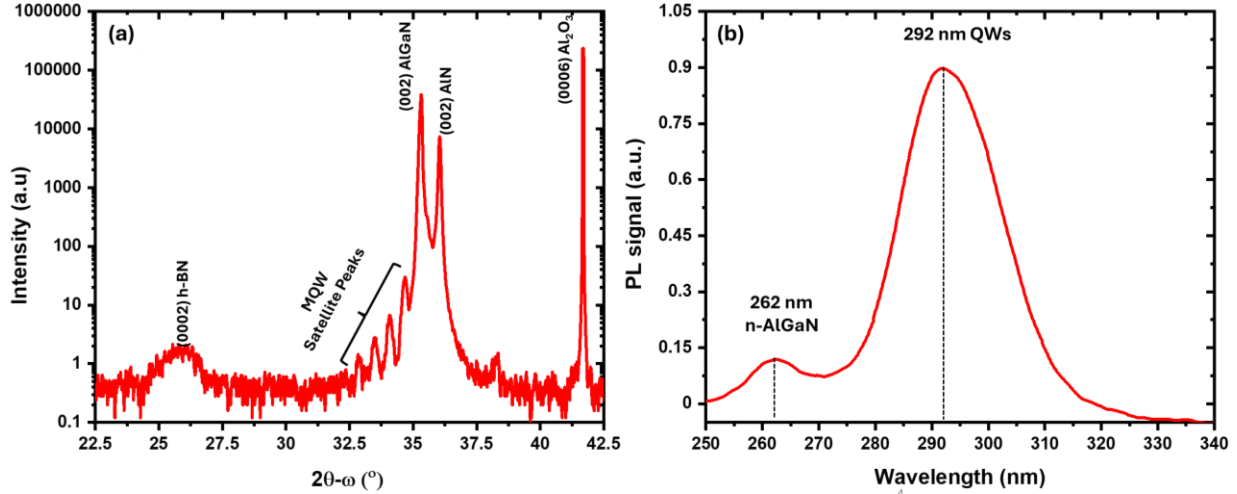


Figure 3. (a) High-resolution triple axis 2θ - ω scan and (b) PL spectrum of the AlGaIn QWs grown on n-AlGaIn/AlN/sapphire.

To determine the emission wavelength of the grown QWs, photoluminescence (PL) measurements were conducted on the samples. The resulting PL spectrum, depicted in Figure 3b, exhibited emission peaks at 262 nm and 293 nm, corresponding to the emission from the QB and QW layers, respectively. The Al composition corresponding to these emission wavelengths was determined by fitting the data using the LDA-1/2 approach [32], yielding values of 0.55 and 0.33 in QB and QW, respectively, which are close to the values obtained by X-Ray diffraction simulation.

2.2 Device Fabrication Process

After the growth and structural characterization, device structures were processed and devices were fabricated. Throughout the fabrication process and upon completion, devices were thoroughly examined using SEM. The analyses confirmed that the top 2-D Mg-doped h-BN layer retained its epitaxial integrity, with no signs of delamination observed. Figure 4a and b shows the

far field image of the processed wafer (inset: optical microscope image of an isolated device) and the schematic of the device design, respectively, on to which further electrical and electroluminescent (EL) characterizations were performed.

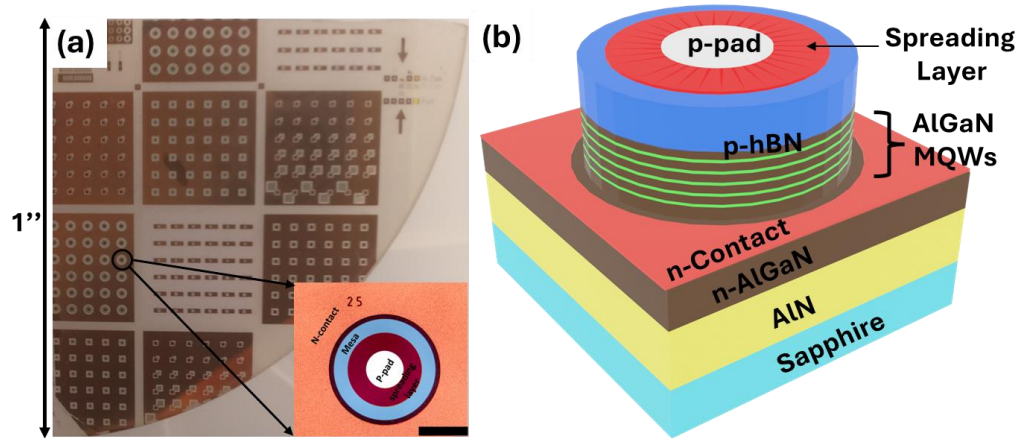


Figure 4. (a) Far field image of processed wafer showing devices. Inset: optical micrograph of a single device, scale bar 200 μm . (b) 3-D schematic of the final fabricated device onto which electrical and EL measurements were performed.

2.3 Electrical and Optical Characterization

Several devices were characterized and representative I-V characteristic are shown in Figure 5a. The devices show significantly lower current in reverse bias and characteristic rectifying behavior. Devices turn on was observed at 7V with forward current of ~ 10 mA at 12V.

Finally, the EL spectrum was recorded at various levels of injected current, as illustrated in Figure 5b. The EL spectrum exhibited a peak at 290 ± 2 nm, in agreement with the PL measurements. A small bump in the EL spectrum at 262 nm was also observed, attributed to the recombination in QBs. Furthermore, a red shift in the emission spectra was observed, as indicated by the green dotted line in Figure 5b, attributable to the band gap narrowing due to self-heating effect^[33], with

increasing injected current values. In addition to UV emission, faint visible orangish emission was also observed from the fabricated devices during EL measurements. This emission could be associated with the recombination originating from carbon defect centers in h-BN, as reported in the literature^[34]. Further investigation will be reported in future work.

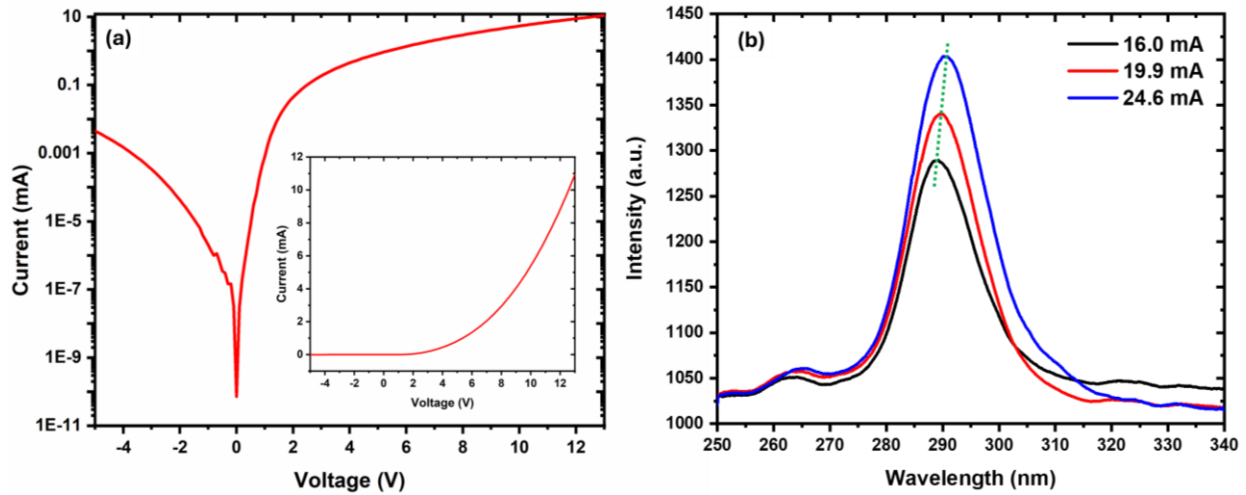


Figure 5. IV curve for the fabricated UV LED and inset showing IV in linear scale. (b) EL spectrum of the fabricated UV LED at different values of injected current.

3. Conclusions

In this study, we report functioning 2-D/3-D UV-LEDs with a Mg-doped h-BN epilayer serving as a hole injection layer. The full structure includes Mg-doped h-BN atop AlGaN MQWs/n-AlGaN grown on an AlN/sapphire template. The devices have characteristic diode rectifying behavior, supporting the formation of a p-i-n junction. Additionally, optical measurements confirm UV emission at wavelengths around 290 nm, proving that h-BN can serve as a hole injection layer.

This proof-of-concept shows the need for much more research into p-doped h-BN as an alternative solution for the p-cladding layer of UV-LEDs and more generally, the need to more fully

understand 2-D/3-D optoelectronic heterostructures. Finally, the fabricated h-BN UV-LEDs point to the potential utility of h-BN as an active material for UV photonics in general.

4. Methods

Growth : Epitaxial growth was performed in an Aixtron Close Coupled Showerhead MOCVD reactor system on 2'' sapphire substrates using hydrogen as carrier gases. Triethylboron (TEB) for boron, trimethylgallium (TEGa) /triethylgallium (TMGa) for gallium, trimethylaluminum (TMAI) for aluminum, and ammonia (NH₃) for nitrogen were used as precursors during the growth process. Silane and bis cyclopentadienyl-magnesium were used as source of Si and Mg atoms for n-type and p-type doping, respectively.

TEM: Cross-sectional lamellae were prepared using focused ion beam (FIB) thinning and ion milling techniques, following the application of a 100 nm thick carbon coating for layer protection. High-angle annular dark-field scanning transmission electron microscopy (HAADF-STEM) was then employed to investigate the structural characteristics at the nanoscale, utilizing an aberration-corrected Thermo Fisher Titan 200 keV electron transmission microscope.

SEM: The SEM was performed, for morphological characterization, using the Zeiss SupraTM 55VP at an EHT of 2.5V with the SE2 detector.

HR-XRD: The HR-XRD measurements were performed in a Panalytical X'pert Pro Materials Research Diffractometer system using Cu K α radiation (Cu K α 1: 1.5405 Å) in the triple-axis mode.

PL: The PL measurements were carried out in a confocal configuration using a Horiba Jobin Yvon instrument with an excitation wavelength of 213 nm and a grating of 600 grooves/mm at room temperature.

Device Fabrication : At first 860 nm thick SiO₂ hard mask was deposited using plasma enhanced chemical vapor deposition, which was patterned using photo resist and etched using 1:7 buffered oxide etchant (BOE) solution. This patterned SiO₂ layer was used as hard mask for mesa etch performed using chlorine/hydrogen chemistry in an induction coupled plasma reactor. After mesa etch SiO₂ hard mask was dissolved in BOE solution and contacts were deposited. Both n-and p-contacts were deposited using standard photolithography and electron beam metallization process. N-contact was made by depositing metal stack consisting of titanium/aluminum/nickel/gold and rapid thermal annealing at 850°C for 30 seconds in nitrogen environment. P-contact was made by depositing nickel/gold stack and annealing it at 650°C for 60 seconds under oxygen environment. Finally, 100 nm thick, p-and n-pads were deposited for probe placements and electrical characterization. All resist strip and metal lift-off were performed in a bath of heated DMSO at 85°C.

EL: EL of the fabricated devices was performed using Keithley 4200A-SCS parameter analyzer on a 2 tip probe station. The EL spectrum of the device was captured from the substrate side by positioning the sample on a custom-made mount and aligning the device with the optical axis of the spectroscope. The device's signal was gathered via a parabolic mirror and recorded using a CCD cooled by Peltier cooling to -74°C. A 1200 grooves/mm grating was utilized for this measurement.

Acknowledgments

A. Perepeliuc, R. Gujrati, P. Vuong contributed equally to this work. This study is partially funded by the French National Research Agency (ANR), under the GANEXT Laboratory of Excellence (LabEx) project and French PIA project Lorraine Université d'Excellence (Grant ANR-15- IDEX-04- LUE).

Conflict of Interest

The authors have no conflicts to disclose.

Data Availability

The data that support the findings of this study are available from the corresponding author upon reasonable request.

Received:

Revised:

Published online:

References

- [1] M. Kneissl, T.-Y. Seong, J. Han, H. Amano, *Nature Photonics* **2019**, *13*, 233.
- [2] M. Kneissl, T. Kolbe, C. Chua, V. Kueller, N. Lobo, J. Stellmach, A. Knauer, H. Rodriguez, S. Einfeldt, Z. Yang, N. M. Johnson, M. Weyers, *Semiconductor Science and Technology* **2011**, *26*.
- [3] F. Mehnke, T. Wernicke, H. Pingel, C. Kuhn, C. Reich, V. Kueller, A. Knauer, M. Lapeyrade, M. Weyers, M. Kneissl, *Applied Physics Letters* **2013**, *103*, 1.
- [4] C. Stampfl, J. Neugebauer, C. G. Van de Walle, *Materials Science and Engineering: B* **1999**, *59*, 253.
- [5] K. B. Nam, M. L. Nakarmi, J. Li, J. Y. Lin, H. X. Jiang, *Applied Physics Letters* **2003**, *83*, 878.
- [6] M. L. Nakarmi, K. H. Kim, J. Li, J. Y. Lin, H. X. Jiang, *Applied Physics Letters* **2003**, *82*,

3041.

- [7] Y. Aoyagi, M. Takeuchi, S. Iwai, H. Hirayama, *Applied Physics Letters* **2011**, 99, 1.
- [8] M. Z. Kauser, A. Osinsky, A. M. Dabiran, P. P. Chow, *Applied Physics Letters* **2004**, 85, 5275.
- [9] S. Heikman, S. Keller, D. S. Green, S. P. DenBaars, U. K. Mishra, *Journal of Applied Physics* **2003**, 94, 5321.
- [10] T. C. Zheng, W. Lin, R. Liu, D. J. Cai, J. C. Li, S. P. Li, J. Y. Kang, *Scientific Reports* **2016**, 6, 1.
- [11] Y. Zhang, S. Krishnamoorthy, J. M. Johnson, F. Akyol, A. Allerman, M. W. Moseley, A. Armstrong, J. Hwang, S. Rajan, *Applied Physics Letters* **2015**, 106.
- [12] S. Zhao, S. M. Sadaf, S. Vanka, Y. Wang, R. Rashid, Z. Mi, *Applied Physics Letters* **2016**, 109.
- [13] D. Liu, S. J. Cho, J. Park, J. Gong, J. H. Seo, R. Dalmau, D. Zhao, K. Kim, M. Kim, A. R. K. Kalapala, J. D. Albrecht, W. Zhou, B. Moody, Z. Ma, *Applied Physics Letters* **2018**, 113.
- [14] H. Ahmad, Z. Engel, C. M. Matthews, S. Lee, W. A. Doolittle, *Journal of Applied Physics* **2022**, 131.
- [15] Y. Taniyasu, M. Kasu, T. Makimoto, *Nature* **2006**, 441, 325.
- [16] T. Kolbe, A. Knauer, J. Rass, H. K. Cho, S. Hagedorn, F. Bilchenko, A. Muhin, J. Ruschel, M. Kneissl, S. Einfeldt, M. Weyers, *Applied Physics Letters* **2023**, 122.

- [17] N. Norimichi, H. Hirayama, T. Yatabe, N. Kamata, *Physica Status Solidi (C) Current Topics in Solid State Physics* **2009**, *6*, 459.
- [18] M. Buonanno, M. Stanislauskas, B. Ponnaiya, A. W. Bigelow, G. Randers-Pehrson, Y. Xu, I. Shuryak, L. Smilenov, D. M. Owens, D. J. Brenner, *PLoS ONE* **2016**, *11*, 1.
- [19] R. J. Drost, B. M. Sadler, *Semiconductor Science and Technology* **2014**, *29*.
- [20] J. Chen, S. Loeb, J. H. Kim, *Environmental Science: Water Research and Technology* **2017**, *3*, 188.
- [21] S. Khan, D. Newport, S. Le Calvé, *Sensors* **2019**, *19*, 5210.
- [22] J. Glaab, N. Lobo-Ploch, H. K. Cho, T. Filler, H. Gundlach, M. Guttmann, S. Hagedorn, S. B. Lohan, F. Mehnke, J. Schleusener, C. Sicher, L. Sulmoni, T. Wernicke, L. Wittenbecher, U. Woggon, P. Zwicker, A. Kramer, M. C. Meinke, M. Kneissl, M. Weyers, U. Winterwerber, S. Einfeldt, *Scientific Reports* **2021**, *11*, 1.
- [23] S. Majety, J. Li, X. K. Cao, R. Dahal, B. N. Pantha, J. Y. Lin, H. X. Jiang, *Applied Physics Letters* **2012**, *100*.
- [24] G. Cassabois, P. Valvin, B. Gil, *Nature Photonics* **2016**, *10*, 262.
- [25] G.-D. Hao, S. Tsuzuki, S. Inoue, *Applied Physics Letters* **2019**, *114*, 0.
- [26] H. X. Jiang, J. Y. Lin, *Semiconductor Science and Technology* **2014**, *29*, 084003.
- [27] A. Mballo, A. Srivastava, S. Sundaram, P. Vuong, S. Karrakchou, Y. Halfaya, S. Gautier, P. L. Voss, A. Ahaitouf, J. P. Salvestrini, A. Ougazzaden, *Nanomaterials* **2021**, *11*, 211.
- [28] P. Vuong, T. Moudakir, R. Gujrati, A. Srivastava, V. Ottapilakkal, S. Gautier, P. L. Voss,

- S. Sundaram, J. P. Salvestrini, A. Ougazzaden, *Advanced Materials Technologies* **2023**, *8*, 1.
- [29] A. Perepeliuc, R. Gujrati, A. Srivastava, P. Vuong, V. Ottapilakkal, P. L. Voss, S. Sundaram, J. P. Salvestrini, A. Ougazzaden, *Applied Physics Letters* **2023**, *122*.
- [30] A. Perepeliuc, R. Gujrati, A. Srivastava, P. Vuong, V. Ottapilakkal, P. L. Voss, S. Sundaram, J.-P. Salvestrini, A. Ougazzaden, In *Oxide-based Materials and Devices XIV* (Eds.: Teherani, F. H.; Rogers, D. J.), SPIE, **2023**, p. 42.
- [31] X. Li, S. Sundaram, Y. El Gmili, T. Ayari, R. Puybaret, G. Patriarche, P. L. Voss, J. P. Salvestrini, A. Ougazzaden, *Crystal Growth & Design* **2016**, *16*, 3409.
- [32] R. R. Pelá, C. Caetano, M. Marques, L. G. Ferreira, J. Furthmüller, L. K. Teles, *Applied Physics Letters* **2011**, *98*.
- [33] E. A. Menkovich, S. A. Tarasov, I. A. Lamkin, S. Y. Kurin, A. A. Antipov, A. D. Roenkov, I. S. Barash, H. I. Helava, Y. N. Makarov, *Journal of Physics: Conference Series* **2013**, *461*, 012027.
- [34] N. Mendelson, D. Chugh, J. R. Reimers, T. S. Cheng, A. Gottscholl, H. Long, C. J. Mellor, A. Zettl, V. Dyakonov, P. H. Beton, S. V. Novikov, C. Jagadish, H. H. Tan, M. J. Ford, M. Toth, C. Bradac, I. Aharonovich, *Nature Materials* **2021**, *20*, 321.

Table of Contents Entry

In this study, we present the fabrication of a novel 2-D/3-D heterostructure diode aimed at producing UV-LEDs. The structure comprises a 2-D p-doped h-BN layer grown atop 3-D AlGaIn MQW/n-AlGaIn epilayers, exhibiting UV emission at 290 nm. These results decisively showcase

the hole injection through p-doped h-BN into AlGaN, offering a proof-of-concept that p-doped h-BN can substitute p-AlGaN, as an alternative hole injection layer, for UV LEDs.

A. Perepeliuc, R. Gujrati, P. Vuong, V. Ottapilakkal, M. T. Thi, M. Bouras, A. Kassem, A. Srivastava, T. Moudakir, G. Patriarche, P. Voss, S. Sundaram, J. P. Salvestrini, and A. Ougazzaden*

Novel 2-D/3-D heterojunction for UV LEDs using Hexagonal Boron Nitride as hole injection

layer.

